International Journal of Fluid Power 5 (2004) No. 1 pp. 7-16

MODELLING AND CONTROL OF PNEUMATIC VANE MOTORS

Peter Beater

Department of Mechanical Engineering - Automation, University of Applied Sciences Südwestfalen,
Lübecker Ring 2, D 59494 Soest, Germany
beater@fh-swf.de

Abstract

There is a broad area of applications where pneumatic vane motors offer unique advantages: high power-to-weight ratio, indifference to overload and stall, cool operation, indifference to dirty or explosive atmospheres. Typically, they are chosen from manufacturers' diagrams such that the torque needed is provided by the motor at the required speed. If necessary, a nozzle is used to reduce speed. Some guidelines have been published about how to design these motors and how to use them in a position control loop, e.g. for robotic applications. This study derives a mathematical model suited to time-domain simulation of the motor, both in an open-loop or closed-loop system. Using geometrical data and the theory of thermodynamic processes the model of an ideal motor is given. In a second step leakage paths and friction are added to describe the behaviour of real motors. This model is implemented in the modelling language Modelica with the help of the domain library PneuLib and used to estimate values for the conductance of the nozzles or the friction terms. Comparisons between the model and measurements are given, both for open-loop and closed-loop operation.

Keywords: reversible pneumatic vane motor, mathematical model, Modelica, PneuLib, PI control, speed control

1 Introduction

Pneumatic drives offer a number of specific advantages: They have an excellent ratio of power to weight, cannot overheat, have a simple design and therefore high reliability and usually a cost benefit. These are the reasons why pneumatic translational drives, i.e. cylinders, are widely used when masses of up to 20 kg have to be transported over ranges of up to 1 m in a short time. The same advantages are true for pneumatic rotational motors.

There are different designs, e.g. gear motors, piston motors or vane motors which are described in greater detail in this paper. Their design is similar to hydraulic motors which have been thoroughly analysed (Ivantysyn and Ivantysynova, 2001). Due to the different properties of air in contrast to mineral oil the behaviour and modelling of pneumatic vane motors differs considerably from that of hydrostatic vane motors.

Section 2 gives an overview of the design and static characteristics of pneumatic vane motors. In the following section the geometry of the working compartments and the thermodynamic processes are discussed. In Section 4 the ideal motor model is developed further and compared with measurements.

In Section 5 the frequency response and control schemes are presented.

This manuscript was received on 06 October 2003 and was accepted after revision for publication on 16 February 2004

2 Principle of Operation

Figure 1 shows the internal construction of a typical reversible vane motor. The eccentrically mounted rotor is fitted into the cylinder. Since the rotor is smaller in diameter and eccentric to the outer chamber, a crescent-shaped chamber is formed, Fig. 3. The vanes in the rotor slots are free to move in and out. Spring or pneumatic loading keeps them flush against the wall of the cylinder during start-up. During operation, centrifugal forces assist in maintaining the seal at the cylinder wall. These vanes divide the chamber into separate compartments, each of different size.

While all other parts are typically made from steel, non-metallic material is used for the vanes. Resin-impregnated, fibre-reinforced materials are the best for general applications, while carbon-reinforced materials are used for heavy duties (see e.g. Wünsch and Mousa, 1987; Barber, 1997).

Compressed air is fed into the cylinder from the rear at port 1 which forces the rotor blades out and the applied force against the vane causes the rotation of the rotor. The compressed air is then evacuated through

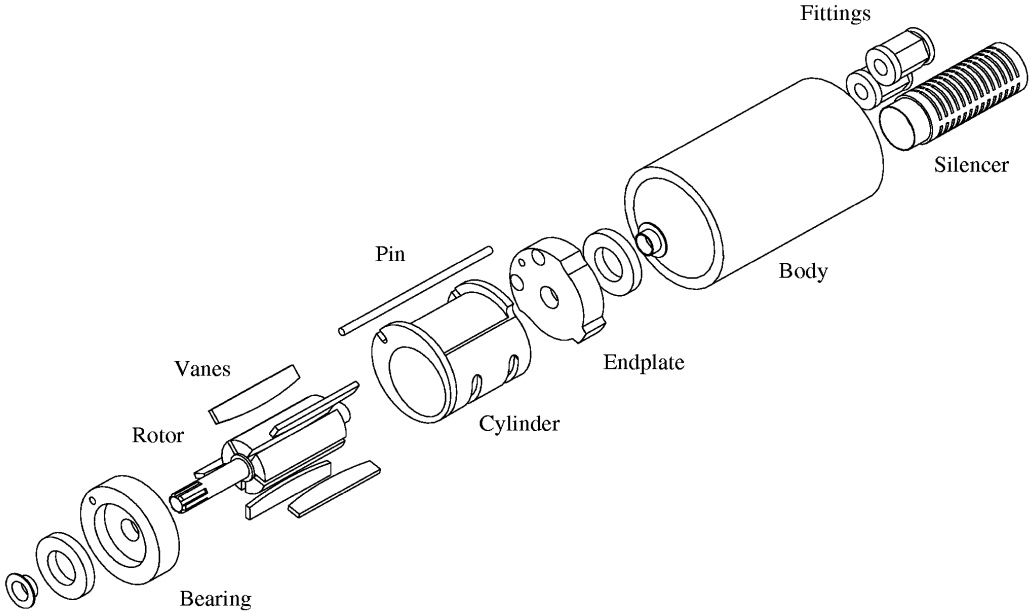

Fig. 1: *Arrangement of reversible vane motor*

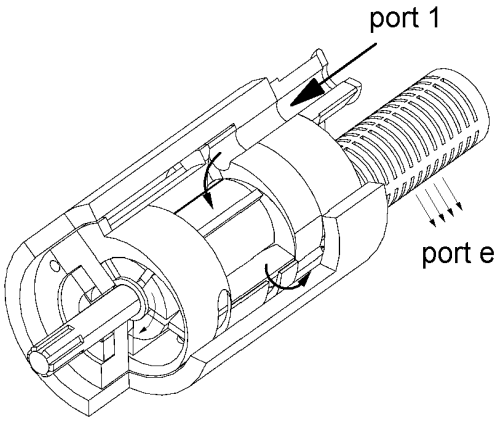

Fig. 2: *Cutaway view and air flow*

holes drilled in the side of the cylinder. The exhaust air passes through the motor body to a silencer at port e and, finally, to atmosphere, Fig. 2.

Exchange of port 1 and 2 is possible for *reversible* vane motors and reverses the direction of rotation of the rotor. *Non-reversible* motors have only port 1 and port e and are designed for one direction of rotation only. They use a non-symmetrical design and can therefore provide a higher output torque. A different design for reversible vane motors that doesn't have an exhaust port is studied by Pu et al (1995).

In former times lubricated air was required to reduce the wear of the vanes. Beginning in the mid-1980's, motors became available that can be operated oil-free (anon., 1985).

Typical designs range from an output power of 80 W, a weight of 300 g and a maximum speed of 13,000 rpm to 18 kW, 53 kg and 6,000 rpm. In handheld tools the maximum speed may be as high as 85,000 rpm. These motors are usually selected from the characteristic curve of torque as a function of speed which is supplied by the manufacturer.

Generally, vane motors produce power patterns similar to those found in series-wound ~~dc~~ motors. At constant inlet pressure, power is zero at 0 rpm, building to a maximum rated power at about 50 % of maximum speed, and then decreasing to zero when the maximum speed is reached.

For the studied motor, Fig. 11 gives the torque and mass flow rate for an absolute supply pressure of 0.73 MPa. The torque decreases linearly with speed. The start-up torque is an important design criterion and given in the manufacturers data sheet. The slope of the torque curve guarantees a stable operation. If the load torque increases, the speed goes down and that leads to a higher torque to balance the load. The maximum power is delivered at half the maximum speed, see Fig. 9. Even for the motor at standstill, there is a substantial air flow that increases with speed, Fig. 11.

3 Mathematical Model

In order to simulate the behaviour of a motor in a digital computer it is necessary to derive a mathematical model. This consists of the equations that describe the geometry, Section 3.1, torque acting on the rotor, Section 3.2, and the mass flow in the motor, Section 3.3. Although the torque can be described by a thermodynamic analysis, there are no simple analytical models for the mass flow. Therefore, a numerical parameter estimation is used.

The model gives mean values for the motor states for a speed range of 25 % to 100 % of the maximum speed and is intended for time domain simulations of complete drive systems or the design of control loops. It doesn't describe the start-up of a motor or the considerable, angle-dependent torque fluctuations (Daser,

1969; Ioannidis, 1987).

For design purposes other models have been developed that describe the internal operation of the motor in detail, e.g. the acting forces on vanes (Schneider, 1994; Ioannidis, 1987; Manuello Bertetto et al, 2002). They can also be adapted to study different designs of rotor or stator (Schneider, 1994; Sbahi, 1992). Design guidelines are given in (Teichmann, 1957; Gerts and Gerts, 1999).

3.1 Geometry of Motor Compartments

To compute the geometric volume of the motor compartments some definitions are given in Fig. 3 and 4 (Sbahi, 1992). The vane angle γ is given by:

$$\gamma = \frac{2\pi}{z} \tag{1}$$

where z: number of vanes, typically between 3 and 8.

The eccentricity ex is the difference between the inner radius of the cylinder and the radius of the rotor:

$$ex = R_S - R_R \tag{2}$$

The rotor angle β is a function of the stator angle α:

$$\beta = \alpha - \arcsin\left(\frac{ex \cdot \sin\alpha}{R_S}\right) \tag{3}$$

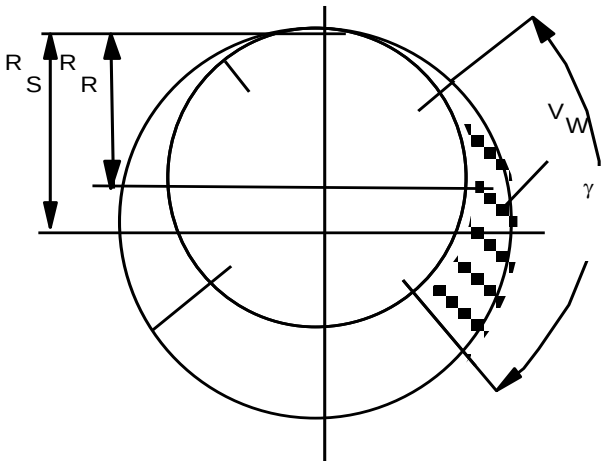

Fig. 3: *Definition of vane angle γ*

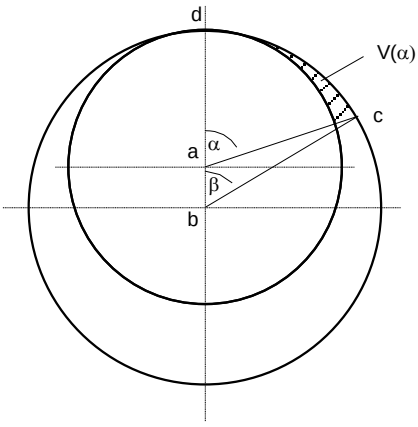

Fig. 4: *Definition of rotor angle α and stator angle β*

The geometric volume of the compartment from point d to point c in Fig. 4 is given by:

$$V_\alpha = \frac{L}{2}(R_S^2 \cdot \beta - R_r^2 \cdot \alpha - ex \cdot R_S \sin\beta) \tag{4}$$

The geometric volume of a working compartment V_w - i.e. the volume between two vanes - is given by:

$$V_w = \begin{cases} V_\alpha & 0 < \alpha \le \gamma \\ V_\alpha - V_{\alpha\text{-}i\gamma} & i\gamma < \alpha \le 2\pi \\ V_{2\pi} - V_{\alpha\text{-}\gamma} & 2\pi < \alpha \le 2\pi + \gamma \end{cases} \quad for \tag{5}$$

Equation 5 can be used to calculate the dead volume V_d, the filling volume V_{fill} and the expanded volume V_{exp} if the geometric data is available, see Fig. 5. The ratio between the expanded and filling volume determines to what extent the internal energy of the air is used and is called the *expansion ratio* ε,

$$\varepsilon = \frac{V_{exp}}{V_{fill}} \tag{6}$$

Brückner (1967) measured values from ε = 1.0 to ε = 1.43 for non-reversible motors. For ε = 1.0 no expansion takes place and this corresponds to gear motors. This means that the internal energy of the air is not used and the exhaust temperature is around ambient temperature. If a high expansion ratio is used, the power of the motor increases but the exhaust temperature can be so low that the water in the supplied air freezes and finally blocks the motor. The nominal displacement volume is given by:

$$V_{disp,nom} = V_{fill} \cdot z \tag{7}$$

In contrast to hydrostatic motors this value is usually not available to customers and therefore not used to select a motor.

3.2 Power and Torque of the Ideal Motor

To derive a mathematical model of the torque the thermodynamic processes are studied. They offer equations to calculate the work which can then be differentiated with respect to time to give the needed model of the power and torque.

Figure 5 shows the volume of one compartment as a function of the rotation angle, Fig. 6 the corresponding *p-V* diagram (assuming clockwise rotation of the rotor). State *a* is the beginning of the rotation when the vane opens the compartment and air fills the dead volume. In state *b* the compartment is completely filled with air of pressure p_1. While the rotor turns to *c* the volume of the compartment increases. This process is assumed to be polytropic, i.e. the air pressure can be calculated by:

$$p_{1\_e} = p_1\left(\frac{V_{exp}}{V_{fill}}\right)^n = p_1\varepsilon^n \tag{8}$$

where

n: polytropic index, $1 \le n \le \kappa$, κ = 1.4 for air.

Typically a value of n = 1.3 is used (Daser, 1969; Sbahi, 1992). When the vane opens, the compartment air leaves and the pressure falls to the surrounding pressure, p_e. This is the pressure at state *d* after the vane

has closed the compartment and a reduction of the compartment volume begins. The air is compressed until at *e* the vane opens and releases most of the air to the second working port. Some air remains, state *f*.

The compression from *d* to *e* is often neglected (e.g. Hannson, 1975; Barth, 1978) but has to be modelled if a speed reduction by throttling at port 2 is to be described by the model.

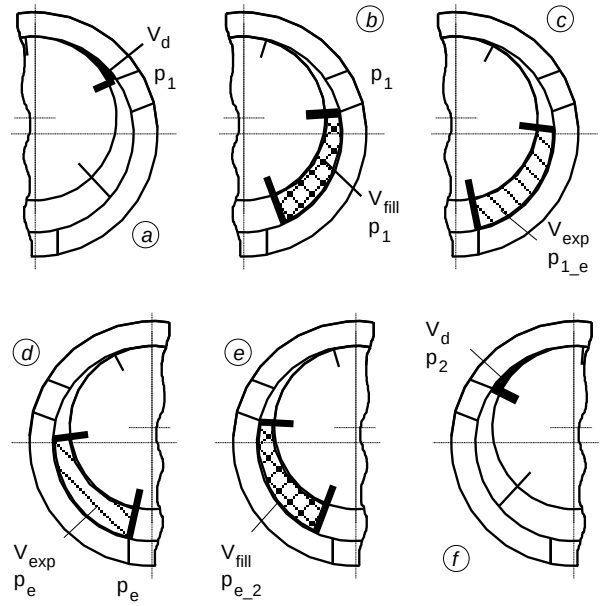

Fig. 5: *Volume of working compartment as a function of rotation angle*

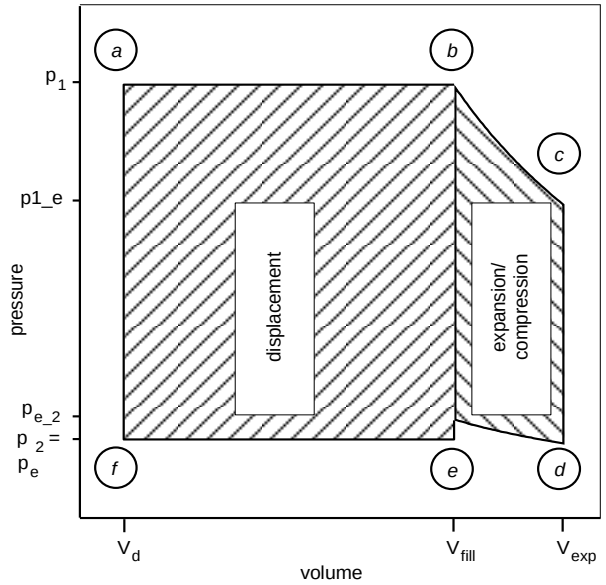

Fig. 6: *p-V diagram*

The work from the whole process is the sum of the expansion work, the displacement work and the compression work. Assuming a polytropic process and an ideal gas the work is given by:

$$W = W_{\text{expansion}} + W_{\text{displacement}} + W_{\text{compression}} \tag{9}$$

$$W_{\text{expansion}} = -\int_{c}^{b} p\,dV = \frac{p_1 V_{\text{fill}}}{\text{n}-1}\left(\varepsilon^{1\text{-n}} - 1\right) \tag{10}$$

$$W_{\text{displacement}} = -\int p\,dV = \left(p_1 - p_2\right)\,\left(V_{\text{fill}} - V_{\text{d}}\right) \tag{11}$$

$$W_{\text{compression}} = -\int_{e}^{d} p\,dV = \frac{p_2 V_{\text{exp}}}{\text{n-1}}\left(\varepsilon^{\text{n-1}} - 1\right) \tag{12}$$

The power *P* of the motor can be calculated by differentiating the work *W* with respect to time. For the simulation model the torque *T* at the motor shaft is needed, which is given by:

$$T = \frac{P}{\omega} = \frac{1}{\omega}\frac{dW}{dt} \tag{13}$$

3.3 Mass Flow

Before the air can enter a compartment it has to flow through long and narrow ducts whose resistance cannot easily be calculated analytically. There is also considerable leakage between the ports and through the bearing at the front side of the rotor. This can be seen in Fig. 11 that shows the mass flow rate. Even at standstill there is a considerable mass flow rate of approx. 65 % of the maximum flow rate.

In Section 3.2 the pressures at the compartment inlets were given as p_1, p_2 and p_e. In a simulation model they have to be computed, however. Therefore, lumped volumes are placed at the three inlets of the stator, see Fig. 7. A differential equation is used to compute the mass and the ideal gas law is used to compute the pressure in that volume. The isothermal approach has been taken because the inherent effect of temperature variation on system dynamics is considered to be negligible when compared with the effects of changes of various other state variables.

$$\dot{m}_1 = \dot{m}_{\text{from\_1}} + \dot{m}_{\text{to\_vol\_1}} \tag{14}$$

$$p_1 = \frac{m_1 \cdot \text{R} \cdot \text{T}_0}{Vol_1} \tag{15}$$

The mass flow rate $\dot{m}_{\text{to\_vol\_1}}$ depends on the pressure at port 1. The mass flow that goes through the motor can be calculated from the compartment volume and the pressure p_1. Assuming clockwise rotation, $\omega > 0$, the mass flow rate from inlet 1 of the stator to inlet *e*, $\dot{m}_{\text{from\_1}}$, is given by:

$$\dot{m}_{\text{from\_1}} = \frac{p_1 \cdot \omega \cdot V_{\text{disp,nom}}}{2\pi \cdot \text{R} \cdot \text{T}_0} \tag{16}$$

For the mass flow rate $\dot{m}_{\text{to\_2}}$, it follows accordingly:

$$\dot{m}_{\text{to\_2}} = \frac{p_{\text{e}} \cdot \omega \cdot \varepsilon \cdot V_{\text{disp,nom}}}{2\pi \cdot \text{R} \cdot \text{T}_0} \tag{17}$$

The mass flow rate $\dot{m}_{\text{to\_e}}$ can be calculated from the fact that the net mass flow must be equal to zero:

$$\dot{m}_{\text{to\_2}} + \dot{m}_{\text{to\_e}} = \dot{m}_{\text{from\_1}} \tag{18}$$

This mathematical model of the ideal motor was implemented with the modelling language Modelica

and included as part of the pneumatics library PneuLib (Pneulib et al, 2003). It describes an ideal vane motor without leakage, inertia or friction. It is similar to specialised models for the design of controllers (Pandian, 1998) but lacks some important features that are needed for time-domain simulation.

In a real motor there are considerable leakage flows, e.g. between the vanes and the stator, and mechanical friction. Therefore, additional flow paths with nozzles, inertia and bearing friction were added to this ideal motor, see Fig. 8 for nozzles.

The nozzle model is based on ISO 6358 with an added laminar flow regimen for a pressure ratio of almost unity. This extension avoids numerical problems that arise due to the infinite gain of the standard equation at this operating point. This extension has already proved very effective for modelling of (incompressible) flow of hydraulic oil through orifices (Beater, 1999). The friction model was taken from the Modelica Standard Library (Modelica 2003).

To find parameter values for the nozzles and the friction model a numerical estimation scheme was used that is described in Section 4.1

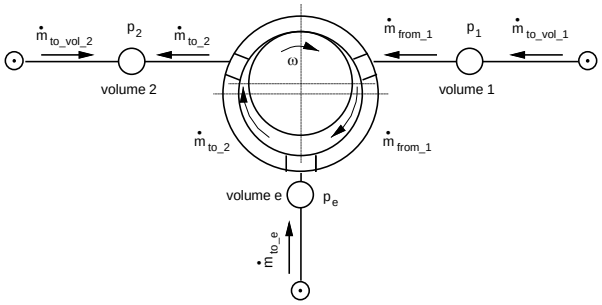

Fig. 7: *Mass flow in the ideal motor*

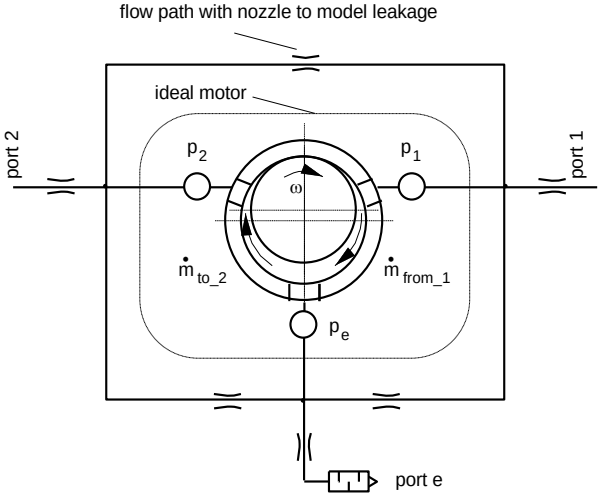

Fig. 8: *Simulation model consisting of ideal motor and leakage flow paths*

3.4 Analysis of Motor Characteristics

The Modelica model can be used to analyse the losses in the vane motor as a function of speed, Fig. 9. There are mechanical losses due to bearing friction and friction between the vanes and the cylinder. This friction could be reduced by using lubricating oil which, however, can cause environmental problems. There are also losses through leakage in the motor. The biggest part are the losses in the ducts leading to and from the working compartments. These losses could be reduced significantly by holes with a greater diameter. In that case some speed controller would be needed to limit the maximum speed of the motor which would otherwise overspeed and destroy itself. This is due to the fact that pneumatic systems are fed by a pressure source that can provide almost unlimited mass flow. Hydrostatic motors are supplied by a flow source and therefore don't face this problem. Pneumatic vane motors with integrated centrifugal controllers are described in the literature (Hansson, 1975; Sbahi, 1992). They have been used in the past for stationary drives but are not offered by most manufacturers today.

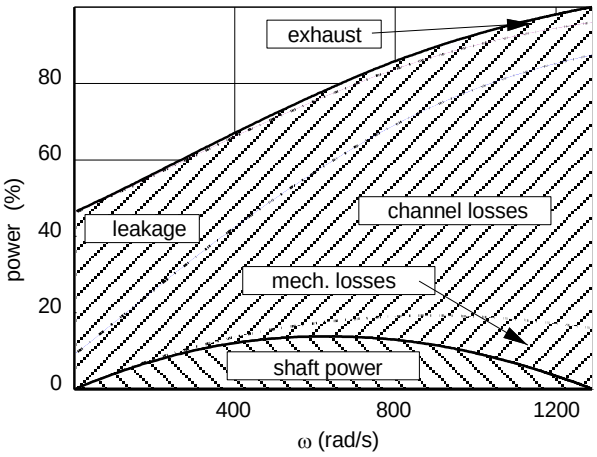

Fig. 9: *Power as a function of angular velocity*

4 Simulation Model and Results

4.1 Object-Oriented Model

The model description language Modelica (Modelica 2003) is based on object oriented modelling which can be described as:

"Ability of a program to represent a physical object regardless of the environment where that object is used".

This leads to the following consequences:

- No causality.
- The models are equation based.
- Model and system have the same structure.

Subsystems are connected through flow- and effort-(across) variables.

The idea is to describe a *component* without looking at the environment in which it will be used later. And that means that it is not defined which variables will be input variables and which output variables in the *complete system*. A simple example is a hydrostatic machine that can be used as a motor and then has pressure and flow rate as input variables while the torque and the speed of the shaft are output variables. In other applications this machine can be used as a pump and then has torque and the speed of the shaft as input variables while pressure and

flow rate are output variables. In both cases the circuit design determines whether it is used as a pump, i.e. converting mechanical energy to hydraulic energy, or motor. Because the input and output variables are not defined when writing the component model but automatically determined when analysing the complete system model this approach is called *non-causal*. The opposite approach is a description by a block diagram. The block oriented way is called *causal* modelling because the input and output variables are defined when writing the component model.

Object-oriented models are *equation based*. They don't use assignment statements as in most higher level programming languages. The force acting on a piston can therefore be described as

$$F - p \cdot A = 0 \tag{19}$$

The symbolic formula manipulation of the object-oriented simulation program solves this equation for the required variable, e.g. the force F as a function of pressure:

$$F = p \cdot A \tag{20}$$

It is very convenient to describe basic effects with equations, e.g. the torque of the ideal motor. When building bigger systems, however, it is easier to do this in the graphical environment ~~that is~~ supplied by the Modelica tools. The connection lines between components are automatically translated into connect statements by the systems such that the complete system is described again by a set of equations.

To couple components – or subsystems – a physical-oriented approach is used in Modelica. Generalising Kirchhoff's laws, *through* and *across variables* are defined. For pneumatic systems this means that there is the through variable mass flow rate, $\dot{m}$, and the across variable pressure, p. At a node, the connection of two or more components, the across variables are identical while the sum of the through variables is zero.

This object-oriented approach makes it possible to build a library of reusable components that can easily be used to model pneumatic systems. In this study the nozzles, reservoirs and mechanical components were taken from the appropriate Modelica libraries. This approach makes it possible to describe the ideal motor with equations and add later graphically the nozzles for the leakage flow or the inertia and bearing friction for the rotating parts. The simulation system automatically solves the resulting equations and computes for instance the flow rate into volume 1 in Eq. 14.

4.2 Parameter Estimation and Results

The simulation model was used to estimate the parameters of the friction and the nozzles that describe the leakage flow in the motor. To do that three reference responses were defined:

- Steady state characteristic of mass flow rate at port 1 and torque as a function of angular velocity ω for constant pressure at port 1.
- Mass flow rates at port 1 and 2 and angular velocity ω as a function of slowly increasing pressure at port 1.
- Mass flow rates at port 1 and 2 and angular velocity ω as a function of slowly decreasing conductance of a variable nozzle at port 2.

The static characteristic was taken from the manufacturer's data sheet. The other responses were measured at the laboratory test rig, Fig. 10. A small vane motor of approx. 100 W was connected via a coupling to an eddy-current brake and a speed pick-up. There were sensors for the reaction torque of the brake, inlet and outlet pressure, mass flow rate and temperature. A 300 W power supply was used as a power source for the brake to provide load steps. The big difference in size between the brake and the vane motor demonstrates the high power-to-volume ratio of these pneumatic drives.

The minimum speed for reference response 2 is about 2900 rpm. This is due to the fact that in this case the pressure is slowly increased starting from atmospheric pressure to 0.73 MPa. It can even happen that the motor doesn't start at all. When using a constant pressure source the minimum speed depends on the load and can be much lower.

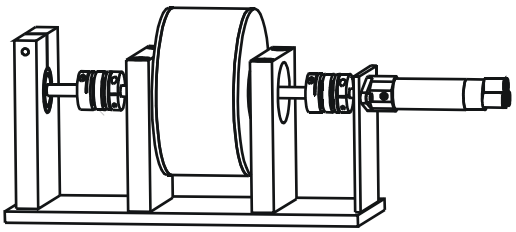

Fig. 10: *Test rig with pneumatic vane motor, brake and speed pick-up*

The reference responses were described by polynomials. The error between them and the computed trajectories was calculated and minimised with the help of an optimisation algorithm. To do that, the tool Dymola (Dynasim, 2003) was used to produce a version of the Modelica model as an executable DOS file. Then the Matlab function *fminsearch* was selected as optimizer. It called another Matlab function that first ran the Modelica model and then computed the error. In order to find a good estimate this procedure was repeated several times with different start values for the optimisation algorithm. This approach was possible because the CPU time for one simulation for reference response 1 takes only 0.11 s on a Pentium 4 processor with 2 GHz. The following figures show some results.

For typical operating conditions, Fig. 11 and 12 show an excellent agreement between the mass flow rate of the model and the reference curve. The error with respect to the torque or speed is acceptable. If the air exiting at port 2 is throttled, the model predicts a reduction in speed but describes the considerable reduction in mass flow poorly, see Fig. 13. This may be due to non-linear effects in the motor which were not modelled.

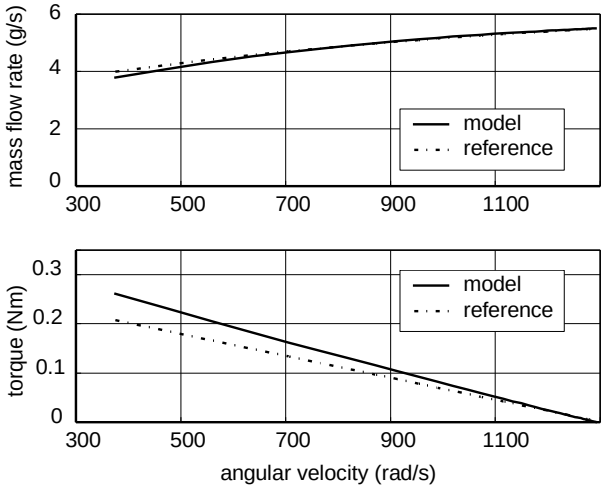

Fig. 11: *Flow rate and torque characteristics of data sheet and simulation model, pressure at port 1 is 0.73 MPa*

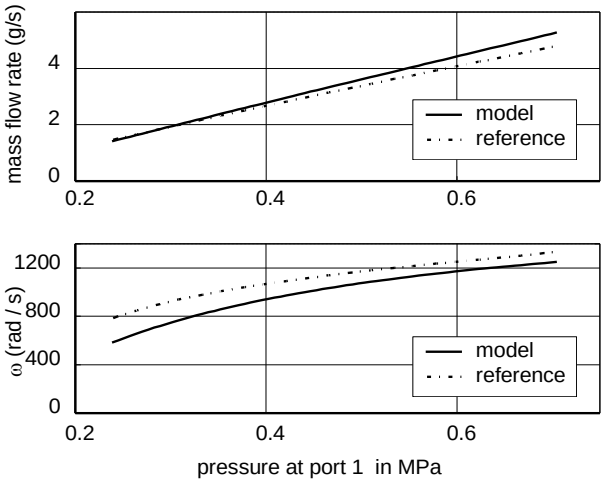

Fig. 12: *Flow rate and speed characteristics of measurement and simulation model, pressure at port 1 varied*

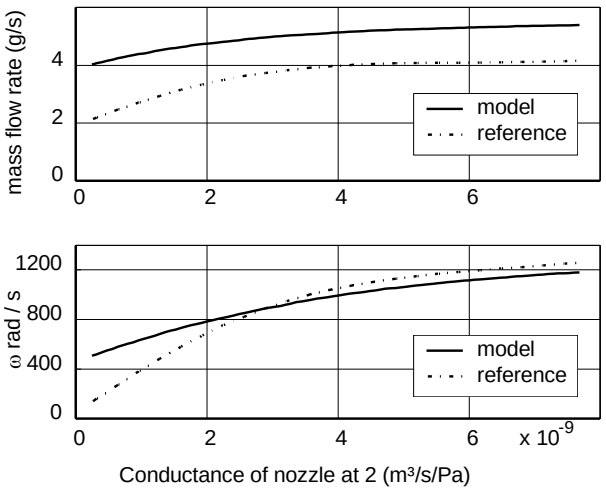

Fig. 13: *Flow rate and speed characteristics of measurement and simulation model, conductance of silencer at port 2 varied*

5 Speed Control

Vane motors are usually chosen in such a way that they offer the required torque at the required speed for the given supply pressure. Often mechanical gears are used to reduce the high speed and typically the manufacturers offer a wide range of integrated gear-boxes.

If necessary the speed can be reduced by lowering the supply pressure, a nozzle at the inlet or outlet port or an electro-pneumatic control system.

Figure 12 shows the effects of a reduced supply pressure. The input mass flow rate and the maximum speed go down. This also limits the stall torque and reduces the starting torque. Section 5.1 shows the effects of throttling and 5.2 gives results for an electro-pneumatic control system.

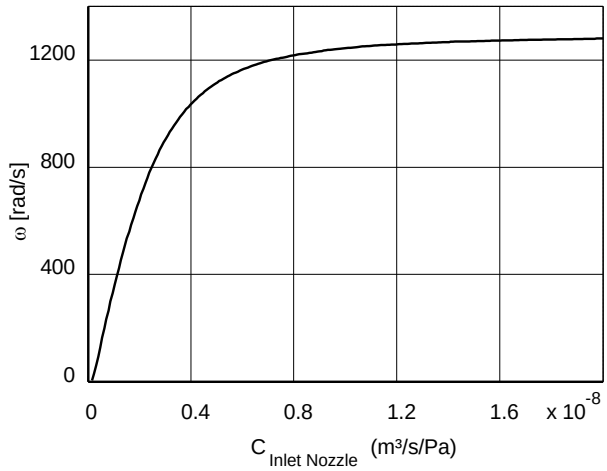

Fig. 14: *Steady-state speed as function of conductance of inlet nozzle*

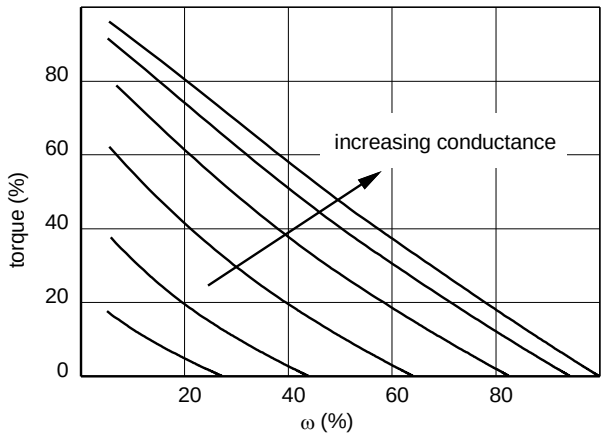

Fig. 15: *Torque versus speed for different inlet nozzles*

5.1 Control by Throttling

One way to reduce the speed is by throttling at the inlet or outlet. Usually this is done at port 1, although it can be fitted at port 2. The following figures show the effect on the steady-state speed and the torque-versus-speed characteristics for throttling at the input using the motor model from Section 4.

5.2 Electro-pneumatic Control Loop

A much more precise speed control can be achieved with an electro-pneumatic control system. In the literature there are some reports about electronically-controlled air motors but typically in position control loops for robot applications. Ioannidis (1987) and Scholz and Schabbel (1987) use modified vane motors and electro-pneumatic servo valves. Noritsugu et al (1987) and Tokhi et al (2001) use radial piston air motors, electro-pneumatic directional valves and PID-controllers. Takemura et al (2000) use a sliding mode controller and find significant steady-state error and tracking error and therefore propose an additional electrical drive to build a hybrid pneumatic/electric motor.

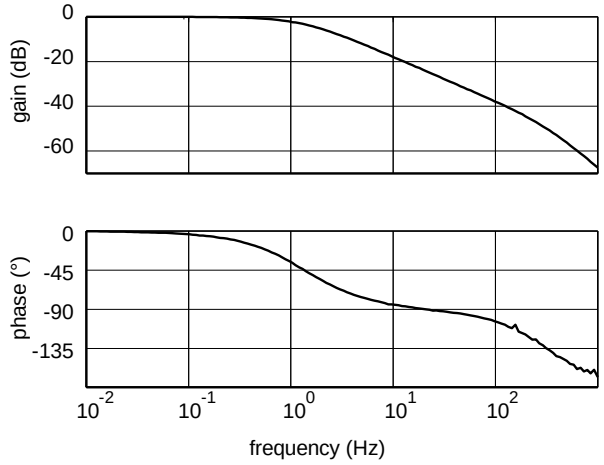

Fig. 16: *Simulated frequency response of motor*

The studied control system consists of an electro-pneumatic pressure control valve, the vane motor with electrical speed pick-up and a digital PI-controller. The electro-pneumatic pressure control valve was chosen for this study because it is much less expensive than a high-quality 5-port, 3-way- directional control valve which can cost much more than the vane motor.

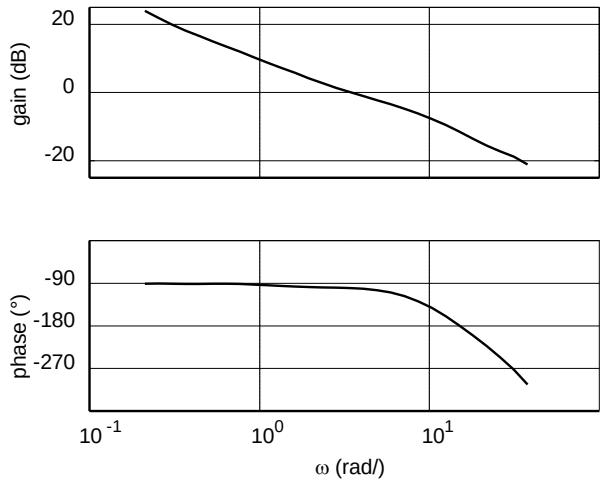

Fig. 17: *Frequency response of open loop system, i.e. pressure control valve and motor*

For the design of the control loop the frequency response of the motor was calculated from the Modelica model and is given in Fig. 16. From a control point of view the motor could be described as two first order systems in series. However, this description is only valid near the used operating point of 0.35 MPa mean pressure and when the motor is not stalled.

The implementation of the designed controller showed, however, that the dynamic response of the used valve cannot be neglected. Therefore, the frequency response of the valve and the motor was measured and used for the design of a PI-controller. The open-loop frequency response is given in Fig. 17.

Figure 18 to 20 show the response of the system. Figure 18 shows a comparison of the response at the test rig and from simulation. For this a simple first-order model was used for the electro-pneumatic valve. Figure 19 gives the responses to a step input for the reference signal, Fig. 20 shows the reaction to a load disturbance. In all cases there is good agreement between measurement and simulation.

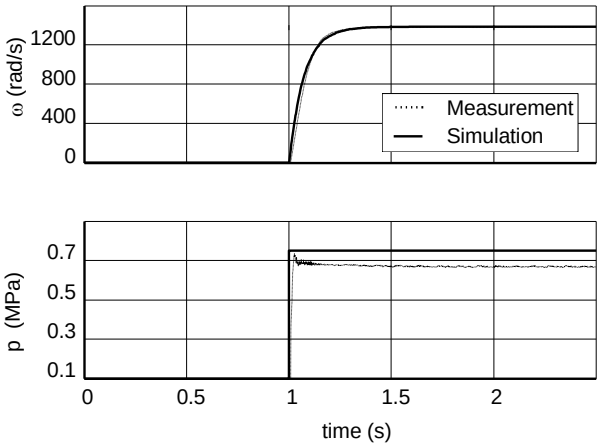

Fig. 18: *Step response of motor and valve*

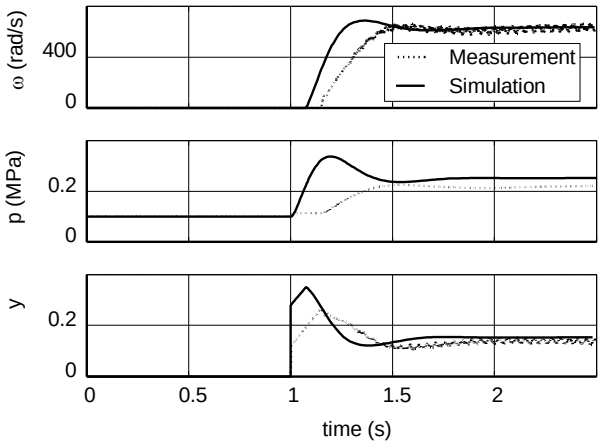

Fig. 19: *Step response of controlled motor*
y input signal to the control valve
p pressure at motor inlet
ω angular velocity of motor

The electro-pneumatic speed control has the unexpected side-effect that the minimum speed of the motor without load is reduced from 2900 rpm without control to 365 rpm with control.

Future work will include the development of a more detailed non-linear valve model to improve the system simulation.

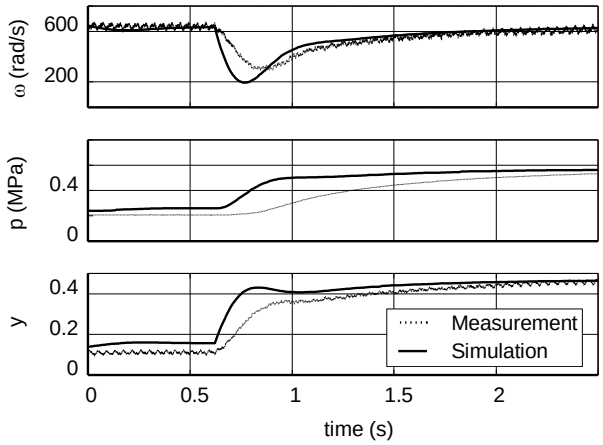

Fig. 20: *Disturbance rejection of controlled system*
y input signal to the control valve
p pressure at motor inlet
ω angular velocity of motor

6 Conclusion

In order to model a reversible vane motor the equations to describe the geometry of the working compartments and the thermodynamic processes were given.

The model was implemented in the language Modelica using PneuLib, a library of pneumatic components in Modelica. The model is included in the library *PneuLibLight* which is freely available (ModelicaLibraries 2003).

Some of the required parameters can be calculated from geometric data while others can only be estimated using the Modelica model and measured responses.

The comparison between measurement and simulation show good agreement for two reference circuits where the input mass flow is varied. A third circuit that has a throttling of output air shows a fair agreement.

An electro-pneumatic speed control loop can be built using the vane motor and a pressure control valve. The controller can be designed using the motor model. A comparison between the simulated closed-loop system and the simulation shows good agreement for several load configurations.

Nomenclature

A	piston area	[m²]
C	sonic conductance of nozzle	[m³/s/Pa]
ex	eccentricity	[m]
F	force	[N]
L	length of rotor	[m]
$\dot{m}$	mass flow rate	[kg/s]
$\dot{m}_1$	net mass flow rate to volume 1	[kg/s]
$\dot{m}_{from\_1}$	mass flow rate from compartment 1	[kg/s]
n	polytropic index	[-]
p	absolute pressure	[MPa]
p_1	absolute pressure entrance compartment 1	[MPa]
p_e	absolute pressure exit compartment 1	[MPa]
P	power	[Nm/s]
R	specific gas constant	[J/kg/K]
R_S	radius of stator (cylinder)	[m]
R_R	radius of rotor	[m]
t	time	[s]
T	torque at motor shaft	[Nm]
T_0	reference temperature	[K]
V	volume of compartment	[m³]
$V_{disp,nom}$	nominal displacement volume	[m³]
V_{exp}	max. volume of compartment	[m³]
V_{fill}	min. volume of compartment	[m³]
W	work	[Nm]
z	number of vanes	[-]
α	rotor angle	[rad]
β	stator angle	[rad]
γ	vane angle	[rad]
ε	expansion ratio	[1]
κ	ratio of specific heat capacities	[1]
ω	angular velocity	[rad/s]

References

anon. 1985. Druckluftmotoren laufen trocken. *VDI Nachrichten*, No. 19, 10 Mai 1985, p. 38.

Barber, A. 1997. *Pneumatic Handbook.* Elsevier Science Ltd., Oxford, UK.

Barth, H. G. 1978. *Druckluft-Drehkolbenmotore - Analyse und Berechnung*. Habilitation TH Clausthal, Germany.

Barth, H. J. 1979. Drehmoment-Verluste durch Ein- und Auslaßdrosselung an Druckluft-Lamellen Motoren. *Ölhydraulik und Pneumatik* 23, pp. 697 – 683.

Beater, P. 1999. *Entwurf hydraulischer Maschinen*. Springer, Berlin Heidelberg New York.

Brückner, W. 1967. *Die Hauptabmessungen nichtumsteuerbarer Druckluft-Lamellenmotoren mit radialer Lamellenanordnung für niedrigen spezifischen Luftverbrauch*. Doctoral thesis, Bergakademie Freiberg, Germany.

Daser, E. 1969. *Das Reaktionsmoment hochtouriger Lamellenmotoren, seine Messung und Bedeutung für die Auslegung der Motoren*. Doctoral thesis, TU Clausthal, Germany.

Dynasim 2003, www.Dynasim.se.

Gerts, E. V. and **Gerts, M. E.**, 1999. Selection of the Parameters of a Reversible Pneumatic Actuator. *Journal of Machinery Manufacture and Reliability*, Vol. 6, pp. 1 – 6.

Hansson, C. 1975. Rotary air motors. In *Atlas Copco Air Compendium*. Atlas Copco AB, Stockholm, Sweden.

Henze, R. 2002. *Betriebseigenschaften und Regelbarkeit pneumatischer Lamellenmotore*. Diploma thesis, FH Südwestfalen, Abt. Soest, Germany, unpublished.

Ioannidis, I. 1987. *Servopneumatische Drehantriebe für Lageregelungen*. Doctoral thesis, RWTH Aachen, Aachen, Germany.

Ivantysyn, J. and **Ivantysynova, M.** 2001. *Hydrostatic pumps and motors*. Akademia Books Int., New Delhi.

Jacazio, G., **Piombo, B.**, **Romiti, A.** and **Sola, A.** 1979. The optimization of the performance of vane-type air motors. *Proceedings to the Fifth World Congress on Theory of Machines and Mechanisms*, Montreal, 1979, Vol. 5, pp. 607 – 609.

Manuello Bertetto, A., **Mazza, L.**, **Pastorelli, S.** and **Raparelli, T.** 2002. A model of contact forces in pneumatic motor vanes. *Meccanica*, Vol 36, pp. 691 – 700.

Modelica 2003. www.modelica.org.

ModelicaLibraries 2003
http://www.modelica.org/libraries.shtml
The model is also included in the demo version of the tool Dymola (Dynasim, 2003).

Noritsugu, T. 1987. Electro-pneumatic feedback speed control of a pneumatic motor: Part I. With an electro-pneumatic proportional valve. *The Journal of Fluid Control*, Vol. 17, pp. 17 – 37.

Pandian, S. R., **Leda, K.**, **Kamoyama, Y.** and **Kawamura, S.** 1998. Modelling and control of a pneumatic rotary actuator. *Proc. Int. Workshop on Power Transmission and Motion Control (PTMC '98),* Bath, England, 1998, pp. 363 – 377.

Pandian, S. R., **Takemura, F.**, **Hayakawa, Y.** and **Kawamura, S.** 1999. Control Performance of an Air Motor - Can Air Motors Replace Electric Motors? *Proc. of the 1999 IEEE International Conference on Robotics & Automation*, Detroit, Michigan, May 1999, pp. 518 – 524.

Pneulib, 2003. www.PneuLib.com

Pu, J., **Wong, C. B.** and **Moore, P. R.** 1995. An Investigation into the Profile Following Capability of Servo-Controlled Air Motors. *4th Scandinavian International Conference on Fluid Power*, Tampere, Finland, pp. 545 – 555.

Sbahi, A. 1992. *Druckluft-Lamellenmotor*. Doctoral thesis, TH Zwickau, Germany.

Schneider, E. 1994. *Optimierung pneumatisch angetriebener Schraubwerkzeuge*. Doctoral thesis, RWTH Aachen, Aachen, Germany.

Scholz, D. and **Schabbel, U.** 1987. Regelungskonzept für Bahnsteuerungen mit Druckluft-Lamellen-motoren. *Ölhydraulik und Pneumatik* 31, No. 9, pp. 688 – 692.

Teichmann, O. E. *1957.* Analysis and design of air motors. *Product Engineering*. Vol. 28, No. 2, pp. 167 – 178.

Tokhi, M. O., **Al-Miskiry, M.** and **Brisland, M.** 2001. Real-time control of air motors using a pneumatic H-bridge. *Control Engineering Practice* 9, pp. 449 – 457.

Wünsch, D. and **Mousa, M.** 1987. Verschleißverhalten von schmierungsfrei betriebenen Druckluft-Lamellen-Motoren. *Antriebstechnik*, Vol. 26, No. 2, pp. 47 – 50.

Appendix

Components used:
Vane motor: Atlas Copco LZB 14 L AR034-11
Pressure control valve: Festo MPPE-3-1/8
Speed pick-up: HÜBNER TDP 0,031 L

Data for motor AR034-11
L = 32e-3 m
R_S = 9e-3 m
R_R = 7.55e-3 m
$V_{disp,nom}$ = 3.8e-6 m³
z = 5
ε = 1.071

Transfer function of PI Controller

$$G(s) = \frac{0.85s + 4}{s}$$

Sonic conductances of the nozzles in the Modelica motor model
C_Nozzle_in_1 = 6.758282e-009 m³/s/Pa
C_Nozzle_EXT = 1.170707e-008 m³/s/Pa
C_Nozzle_out_2 = 6.758282e-009 m³/s/Pa
C_Nozzle_1_Ext = 2.077886e-009 m³/s/Pa
C_Nozzle_2_Ext = 2.077886e-009 m³/s/Pa
C_Nozzle_1_2 = 7.616275e-010 m³/s/Pa

The values for C_Nozzle_in_1 and C_Nozzle_out_2 have the same magnitude as a pneumatic line with the geometric data of the channels to and from the working chambers (round bore, diameter 2 mm, length 8 mm). The value for C_Nozzle_EXT has the same magnitude a nozzle that describes the leakage flow at standstill (0.73 MPa absolute pressure, mass flow rate of 1.8 g/s).

Peter Beater
Dr. Peter Beater is professor at the department of mechanical engineering - automation of the University of Applied Sciences Südwestfalen in Soest, Germany. He obtained his diploma degree (Dipl.-Ing.) from the Technische Universität Braunschweig, Germany, in 1985 and his doctoral degree (Dr.-Ing.) from the Ger-hard-Mercator - Universität Duisburg, Germany, in 1987. His research interests are in modelling, simulation and control of fluid power drives. He is a personal member of the Modelica Asscociation, Linköping, Sweden, and of the International Editorial Board of this journal.